CrystEngComm

COMMUNICATION

Ti³⁺:TiO₂/TiF₃ hybrid with enhanced visible-light photocatalytic reactivity

Xiaodong Meng,[a] Baibiao Huang,[*a] Xiangchao Ma,[b] Zeyan Wang,[*a] Zhaoke Zheng,[a] Junpeng Wang,[a] Xiaoyan Qin,[a] Xiaoyang Zhang[a] and Ying Dai[b]

Ti³⁺:TiO₂/TiF₃ hybrid was synthesized via a one-step facile solvothermal method. Due to the existence of TiF₃, TiO₂ contained high concentration of Ti³⁺ species and Ti³⁺ was stabilized. Ti³⁺:TiO₂/TiF₃ hybrid exhibited excellent visible-light photocatalytic reactivity. The electron structure of TiF₃ was studied, and the photocatalytic mechanism was also proposed.

Photocatalysis is a promising solar energy conversion technique and an effective way to decompose organic contaminants, which has been tremendously investigated in the past decades since Fujishima and Honda reported the photoelectrochemical water-splitting on a TiO₂ electrode.[1] Although great progresses have been made, the low efficiency still fails to meet the requirement for practical applications. The poor visible light absorption and the rapid recombination of photogenerated charge carriers are regarded as two main problems that affect the photocatalytic efficiencies.[2] Therefore, both of the above problems should be addressed for high efficient photocatalyst.

TiO₂ is one of the most investigated photocatalysts due to its unique chemical and physical properties such as high stability and photocatalytic activity.[3-4] However, it can only work under ultraviolet irradiation because of its wide band gap. Various methods have been used to further extend its light absorption spectrum such as metal or/and non-metal doping.[5-6] However, those methods would inevitably introduce some impurity ions, which could probably act as recombination centers and then lower the photocatalytic efficiency.[7] Furthermore, the doping concentrations are usually low, which leads to weak visible light absorptions.

Recently, Zuo et al. reported that Ti³⁺ doping can effectively enhance the visible light absorption of TiO₂ and then enhance the photocatalytic efficiency.[8] However, Ti³⁺ species is not stable since it can be easily oxidized. Therefore, developing a facile strategy to synthesize TiO₂ with stabilized Ti³⁺ is still a great challenge. In the past years, several methods were proposed to increase the concentration of Ti³⁺ and improve its stabilization. Mao et al. reported a black hydrogenated titanium dioxide nanocrystal with strong visible-light photocatalytic reactivity.[9] However, the hydrogenation procedure demands high temperature and long reaction time, which is impractical for application usage. Ju et al.

proposed that F⁻ can stabilize Ti³⁺ species in TiO₂ and then enhance its visible photocatalytic reactivity[10], which offered a new strategy to synthesize Ti³⁺ doped TiO₂ by a readily process.

On the other hand, besides the investigations on extending the light absorption range of TiO₂ by Ti³⁺ doping, it is also important to improve the charge separation efficiency. Previous researches have demonstrated that constructing hybrid is an effective way to promote the separation and many kinds of TiO₂ hybrids such as Ag₂O/TiO₂, Bi₂WO₆/TiO₂ have been certified to possess improved photocatalytic reactivity.[11-12] Based on previous research, hybrid could effectively deter the recombination of excited electron-holes and then can be used to improve the photocatalytic performance of Ti³⁺ doped TiO₂.

Herein, we report a novel Ti³⁺:TiO₂/TiF₃ hybrid synthesized via a one-step solvothermal procedure. By controlling the amount of metal Zn added, Ti³⁺:TiO₂/TiF₃ samples (different molar ratio of Zn and Ti added, R_{ZT}=Zn:Ti) with different TiF₃/TiO₂ ratios can be readily obtained. Owing to the existence of TiF₃ and the hybrid structure, Ti³⁺:TiO₂/TiF₃ samples exhibit enhanced photocatalytic activity under visible light irradiation (λ≥420nm), which could be attributed to the synergistic effects of the high concentration of Ti³⁺ in TiO₂ and the improved charge separation.
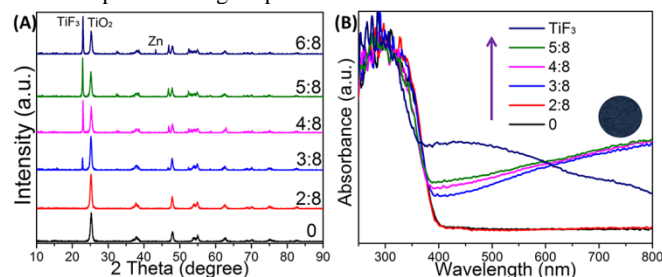
Fig. 1 (A) XRD patterns and (B) UV-Vis diffuse reflectance spectra of Ti³⁺:TiO₂/TiF₃ samples obtained with different ratios (R_{ZT}) of Zn and Ti (inset: photograph of the sample with R_{ZT}=4:8).

The structures of the as-prepared samples were firstly characterized by X-ray diffraction (XRD). As shown in Fig. 1A, the samples without the addition of Zn and that with R_{ZT}=2:8 were pure phase of anatase TiO₂ (JCPDS No.21-1272). As the amount of Zn increased in the starting materials, diffraction peaks corresponding to

TiF$_3$ (JCPDS No. 75-149) appeared which gradually became stronger with the increase of Zn. Besides the diffraction peaks of anatase TiO$_2$ and TiF$_3$, metallic Zn peaks were also detected for the sample with R$_{ZT}$=3:4, which could be due to the excessive Zn during the reaction.

Although Zn was added into this reaction system, no zinc peaks were observed in the XRD patterns for the samples with R$_{ZT}$≤5:8. X-ray photoelectron spectroscopy (XPS) was employed to further investigate whether Zn existed in the as-prepared samples. As shown in the Zn 2p XPS spectra (Fig. S2 in ESI†), no peaks can be detected for the samples with R$_{ZT}$ ratios from 2:8 to 5:8, which indicates that no Zn element existed in our samples and Zn only acted as a reducing agent during the reaction. This result differs from that we reported previously, where Zn was found to act as a stabilizer of Ti^{3+} in the form of ZnO. This difference could be attributed to the introduction of TiF$_4$, which could release F$^-$ during the reaction and produce a more acidic environment. As a result, ZnO could be dissolved and no longer acted as the Ti^{3+} stabilizer. Instead, as reported before, F$^-$ ions will help stabilize Ti^{3+} and then increase the concentration of Ti^{3+} in TiO$_2$.[10]

The color of the above samples changed a lot by varying the R$_{ZT}$ values. As shown in the diffuse reflectance spectra (DRS) in Fig. 1B, the samples of pure anatase TiO$_2$ only have light absorption in the UV region with an absorption edge at ca. 400 nm. The samples containing both anatase TiO$_2$ and TiF$_3$ exhibited additional absorption in visible light region with an upward tail, which was totally different from that of TiF$_3$. Although TiF$_3$ also had a strong absorption in visible region, its absorption intensity gradually decreased with the increase of wavelength. It has been proven that Ti^{3+} species in TiO$_2$ can cause photo-excitation in the IR region.[13] The measured optical absorption spectra and the calculated data[14] both showed an increasing absorption tail as λ>400 nm. Therefore, the visible light absorption of TiO$_2$/TiF$_3$ samples was induced not only by TiF$_3$ but also by the Ti^{3+} species in TiO$_2$.
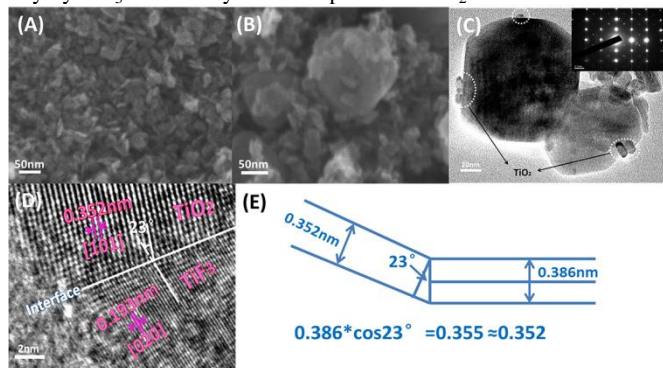

Fig. 2 SEM images of Ti^{3+}:TiO$_2$/TiF$_3$ with (A) R$_{ZT}$=2:8 and (B) R$_{ZT}$=4:8. (C, D) the HR-TEM images of Ti^{3+}:TiO$_2$/TiF$_3$ with R$_{ZT}$=4:8 (inset: SAED pattern of TiF$_3$). (E) Schematic diagram illustrating the lattice matching between TiO$_2$ and TiF$_3$ in Ti^{3+}:TiO$_2$/TiF$_3$ hybrid.

The morphologies of the as-prepared samples were characterized by scanning electron microscopy (SEM). As shown in the SEM image in Fig. 2A, the sample with R$_{ZT}$=2:8 consisted of small nanoparticles with sizes of 10 to 20 nm. While Ti^{3+}:TiO$_2$/TiF$_3$ sample with R$_{ZT}$=4:8 (Fig. 2B) consisted of particles with different sizes, where the smaller particles should be anatase TiO$_2$ and the bigger ones should be TiF$_3$ compared with that from Fig. 2A. This assumption was later confirmed by HR-TEM images as shown in Fig. 2C and 2D. The particles with different sizes were attached tightly with each other and the inset SAED pattern of the bigger particles confirmed the rhombohedral crystal structure of TiF$_3$. For a

closer observation, the lattice spacing of 0.352 nm and 0.193 nm were observed in Fig. 2D, which can be attributed to the (101) atomic planes of TiO$_2$ and (020) atomic planes of TiF$_3$, respectively. And the angle between the two planes was 23°. As illustrated in Fig. 2E, the (101) atomic planes of TiO$_2$ were closely connected to the (010) atomic planes of TiF$_3$ through an angle of approximately 23°, which means TiO$_2$ and TiF$_3$ particles were joint by lattice matching.[15] The intimate contact between TiF$_3$ and TiO$_2$ would facilitate the charge transfer between them and then enhance the photocatalytic efficiency.
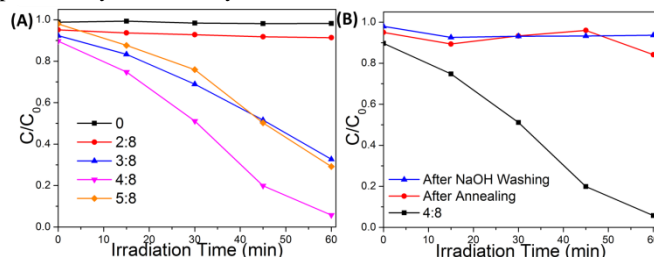

Fig. 3 (A) Photodegradation of MO over Ti^{3+}:TiO$_2$/TiF$_3$ hybrids obtained with different R$_{ZT}$ under visible-light irradiation (λ≥420 nm). (B) Photodegradation of MO of Ti^{3+}:TiO$_2$/TiF$_3$ sample obtained with R$_{ZT}$=4:8 before, after annealing, after alkali washing under visible-light irradiation (λ≥420 nm).

The photocatalytic properties for the samples were evaluated by the photodegradation of methyl orange (MO) under visible light irradiation (Fig. 3A). The samples of pure anatase TiO$_2$ exhibited little photocatalytic performance due to the absence of visible light absorption. As for Ti^{3+}:TiO$_2$/TiF$_3$ samples, they all exhibited excellent photocatalytic performance under visible light irradiation due to their strong visible light absorption, among which the sample with R$_{ZT}$=4:8 showed the highest photocatalytic reactivity and could completely degrade methyl orange molecules within one hour. Although sample with R$_{ZT}$=5:8 contained higher amount of TiF$_3$, it can only degrade 70% of MO within one hour due to the relatively weaker capacity of absorbing MO molecules compared to sample with R$_{ZT}$=4:8, which is beneficial to the photocatalytic reactions.[16]

In order to further understand the roles of Ti^{3+} and TiF$_3$ during the photocatalytic procedure, two comparison tests were carried out. Ti^{3+}:TiO$_2$/TiF$_3$ samples with R$_{ZT}$=4:8 were annealed to remove the Ti^{3+} species in TiO$_2$ (Fig. S4 in ESI†) and washed in alkaline solution to remove TiF$_3$ (Fig. S5 in ESI†). Both processed samples showed decreased photocatalytic activity (Fig. 3B). As TiF$_3$ was removed from the Ti^{3+}:TiO$_2$/TiF$_3$ hybrid, only Ti^{3+}:TiO$_2$ remained. However, the poor photocatalytic performance could be attributed to the relatively high Ti^{3+} concentrations in Ti^{3+}:TiO$_2$, which could became recombination centres for photogenerated charge carriers and lower the photocatalytic activity. On the other hand, TiO$_2$/TiF$_3$ hybrid after removing Ti^{3+} by annealing also exhibited poor visible light activities, even if TiF$_3$ could absorb visible light. This indicates TiF$_3$ could be photo inactive due to its special electronic structures. And both Ti^{3+} and TiF$_3$ are critical important for the visible light photocatalytic performance of Ti^{3+}:TiO$_2$/TiF$_3$ hybrid. Ti^{3+} in TiO$_2$ mainly contributes to the visible light absorption to generate electron-hole pairs, and TiF$_3$ could only facilitate the charge separation, which synergistically improves the visible light photocatalytic activity of the hybrid.
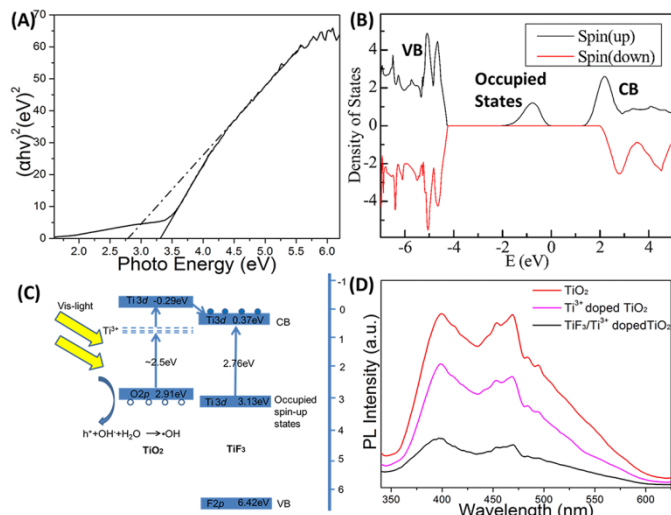
Fig. 4 (A) Plot of $(\alpha h\nu)^2$ vs photon energy (hv) for TiF$_3$, (B) DOS plot calculated for TiF$_3$, (C) Schematic diagram illustrating the photocatalytic process of Ti^{3+}:TiO$_2$/TiF$_3$ hybrid. (D) Photoluminescent spectra (PL) of pure anatase TiO$_2$, Ti^{3+} doped TiO$_2$, Ti^{3+}:TiO$_2$/TiF$_3$ hybrid with the excitation of 320nm.

The band gap of TiF$_3$ is determined from the plot of $(\alpha h\nu)^2$ vs photon energy (hv) due to its direct transition based on our band structure calculations (Fig. 4A).[17] The plot demonstrates two band gap energies of 2.76 eV and 3.3 eV, which means that two band gaps exist in TiF$_3$. In order to better understand the unusual absorbance of TiF$_3$, DFT calculations are employed as shown in Fig. 4B. The result demonstrates that the spin-up density of states (DOS) and spin-down DOS are asymmetric. To be specific, the spin-down states are consistent with common semiconductor with an energy gap of about 6.0 eV between the valence band maximum and conduction band minimum. However, for the spin-up states, some gap states (occupied spin-up states) appear in the band gap and the Fermi level is located just above those states. That is to say electrons in the occupied spin-up states can actually be excited into the conduction band (CB). For the electrons in the valence band, they can be excited either to occupied spin-up states or CB by photons with energies of 2.2 eV or 5.8 eV, respectively. In general, the calculated band gaps are underestimated. Therefore, it is reasonable to believe that the transition of 3.3 eV (Fig. 4A) is from the valence band to occupied spin-up states and the transition of 2.76eV is from occupied spin-up states to CB. Since the Ti 3d states, which form the occupied spin-up states, is very localized, the inactiveness of the photocatalytic activity of TiF$_3$, as observed experimentally, is probably attributed to the weak mobility of photogenerated holes in the initially occupied spin-up states.

According to the aforementioned experimental and theoretical results, a plausible photocatalytic mechanism was proposed as illustrated in Fig. 4C. The position of VB, occupied spin-up states and CB of TiF$_3$ are determined by Anderson's rule[18] (calculation details in ESI†). Under visible light irradiation, electrons in localized Ti^{3+} states in TiO$_2$ are firstly excited into the conduction band according to the light absorption in visible and near-infrared of Ti^{3+} species. Since there are holes in localized Ti^{3+} states upon their excitation, photogenerated electron-hole pairs can also be formed due to the excitation from the VB of TiO$_2$ to the localized Ti^{3+} states with band gap of about 2.5 eV.[19] Then the corresponding holes would form hydroxyl radical (•OH), which is an important oxidative species during the degradation of organic contaminant.[20] On the other hand, since the CB of TiO$_2$ is more negative than the CB of TiF$_3$, the electrons would migrate to the CB of TiF$_3$. In this way, the

photogenerated electrons and holes were effectively separated. Furthermore, the close interfaces between TiO$_2$ and TiF$_3$ through lattice matching could also facilitate the charge transfer between TiO$_2$ and TiF$_3$. Thus, the photocatalytic efficiency is improved.

In a typical photocatalytic reaction, the efficiency is greatly influenced by the rapid recombination of photogenerated electrons-holes. Since the photoluminescence (PL) emission spectrum is the direct result of the recombination of the charged carriers, it is an effective approach to investigate the recombination rate of carriers in our samples. Fig. 4D presents a comparison of the PL spectra of different samples with the excitation of 320 nm. Two main emission peaks of TiO$_2$ appear at about 396 nm (3.13 eV) and 465 nm (2.67 eV). The former one is caused by the emission of band gap transition with the energy of light which is approximately equivalent to the band gap energy of anatase and the latter one is attributed to the charge transition from Ti^{3+} to oxygen anions in a TiO$_6^{8-}$ complex.[21] Pure anatase TiO$_2$ exhibited the highest PL intensity which indicates that it has the greatest carrier recombination rate in the three samples. Ti^{3+} doped TiO$_2$ showed relatively low PL intensity due to the Ti^{3+} species. The PL intensity of Ti^{3+}:TiO$_2$/TiF$_3$ sample revealed a significant decrease compared with pure anatase TiO$_2$ and Ti^{3+} doped TiO$_2$, which means that Ti^{3+}:TiO$_2$/TiF$_3$ hybrid has indeed lowered the recombination rate of electrons and holes, as proposed theoretically.

Conclusions

In summary, we demonstrated a simple solvothermal method to synthesize Ti^{3+}:TiO$_2$/TiF$_3$ hybrid. The Ti^{3+}:TiO$_2$/TiF$_3$ samples showed significant absorption in visible-light region and exhibited enhanced photocatalytic reactivity under visible-light irradiation. With the increase of metal Zn added, the photctalytic reactivity increased and then declined. The Ti^{3+}:TiO$_2$/TiF$_3$ sample with R$_{ZT}$=4:8 showed the best degradation properties. The enhanced photocatalytic performance was attributed to the high concentration of Ti^{3+} species in TiO$_2$ and the effective charge transfer between the TiF$_3$ and TiO$_2$. Our work provides a new strategy to further enhance the photocatalytic reactivity of Ti^{3+} doped TiO$_2$ by constructing hybrid.

Notes and references

[a] State key Laboratory of Crystal Materials, Shandong University, Jinan 250100, China, Email: bbhuang@sdu.edu.cn, wangzeyan@sdu.edu.cn;

[b] School of Physics, Shandong University, Jinan 250100, China

† Electronic Supplementary Information (ESI) available: Experimental details, XRD pattern, XPS spectra, UV-Vis absorption spectra, DET calculation details. See DOI: 10.1039/c000000x/

1 A. Fujishima, K. Honda, *Nature*, 1972, **238**, 37.

2 J. W. Tang, J. R. Durrant, D. R. Klug, *J. Am. Chem. Soc.*, 2008, **130**, 13885.

3 Y. Li, T. Sasaki, Y. Shimizu, N. Koshizaki, *J. Am. Chem. Soc.*, 2008, **130**, 14755–14762.

4 Y. Li, T. Sasaki, Y. Shimizu, N. Koshizaki, *Small,* 2008, **4**, 2286–2291.

5 W. Choi, A. Termin, M. R. Hoffmann, *J. Phys. Chem.*, 1994, **98**, 13669.

6 R. Asahi, T. Morikawa, T. Ohwaki, K. Aoki, Y. Taga, *Science*, 2001, **293**, 269.

7 R. Vogel, P. Hoyer, H. Weller, *J. Phys. Chem.*, 1994, **98**, 3183.

8 F. Zuo, L. Wang, T. Wu, Z. Y. Zhang, D. Borchardt, P. Y. Feng, *J. Am. Chem. Soc.*, 2010, **132,** 11856–11857.

9 X. B. Chen, L. Liu, P. Y. Yu, S. S. Mao, *Science*, 2011, **331,** 746.

10 J. C. Yu, J. G. Yu, W. K. Ho, Z. T. Jiang, L. Z. Zhang, *Chem. Mater.*, 2002, **14**, 3808-3816.

11 W. J. Zhou, H. Liu, J. Y. Wang, D. Liu, G. J. Du, S. J. Han, J. J. Lin, R. J. Wang, *Phys. Chem. Chem. Phys.*, 2010, **12**, 15119–15123.

12 J. Tian, Y. H. Sang, G. W. Yu, H. D. Jiang, X. N. Mu, H. Liu, *Adv. Mater.*, 2013, **25**, 5075-5080.

13 L. Schlapbach, A. Züttel, *Nature*, 2001, **414**, 353.

14 Z. S. Lin, A. Orlov, R. M. Lambert, M. C. Payne, *J. Phys. Chem. B,* 2005, **109**, 20948.

15 T. Watanabe, H. Funakubo, K. Saito, T. Suzuki, M. Fujimoto, M. Osaka, Y. Noguchi, M. Miyayama, *Appl. Phys. Lett.,* 2002, **81**, 1660.

16 Z. K. Zheng, B. B. Huang, X. D. Meng, J. P. Wang, S. Y. Wang, Z. Z. Lou, Z. Y. Wang, X. Y. Qin, X. Y. Zhang, Y. Dai, *Chem. Commun.*, 2013, **49**, 868-870.

17 X. Zhang, Z. H. Ai, F. L. Jia, L. Z. Zhang, *J. Phys. Chem. C,* 2008, **112**, 747-753.

18 A. Walsh, K. T. Butler, *Acc. Chem. Res.,* 2014, **47,** 364-372.

19 Q. Zhu, Y. Peng, L. Lin, C. M. Fan, G. Q. Gao, R. X. Wang, A. W. Xu, *J. Mater. Chem. A,* 2014, **2** 4429–4437.

20 H. Lachheb, E. Puzenat, A. Houas, M. Ksibi, E. Elaloui, C. Guillard, J. M. Herrmann, *Appl. Catal. B- Environ.,* 2002, **39,** 75–90.

21 Z. K. Zheng, B. B. Huang, J. B. Lu, X. Y. Qin, X. Y. Zhang, Y. Dai, *Chem. Eur. J.*, 2011, **17**, 15032-15038.

Ti³⁺:TiO₂/TiF₃ hybrid with enhanced visible-light photocatalytic reactivity

Xiaodong Meng,[a] Baibiao Huang,[*a] Xiangchao Ma,[b] Zeyan Wang,[*a] Zhaoke Zheng,[a] Junpeng Wang,[a] Xiaoyan Qin,[a] Xiaoyang Zhang[a] and Ying Dai[b]
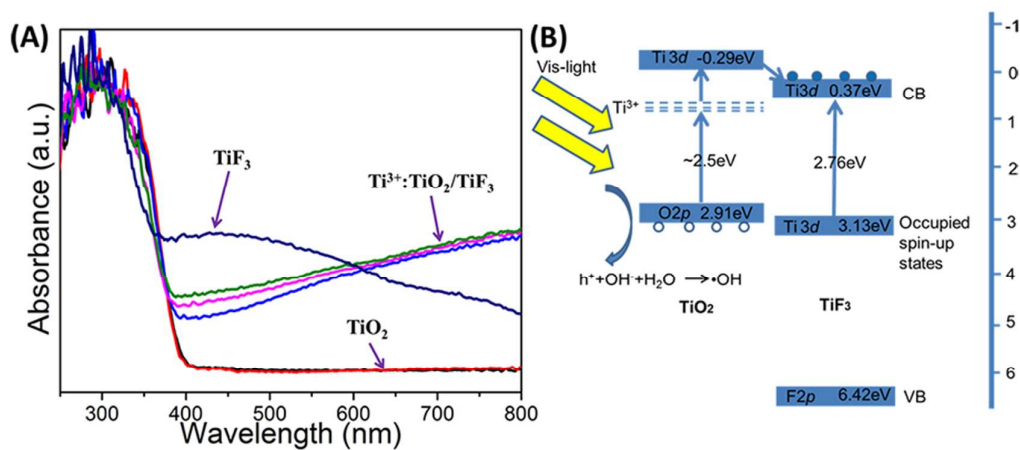
Ti³⁺:TiO₂/TiF₃ hybrid contains high concentration of Ti³⁺ species and exhibits enhanced absorption in visible region.